Chemosphere 332 (2023) 138807

Contents lists available at ScienceDirect

Chemosphere

journal homepage: www.elsevier.com/locate/chemosphere

Leaching of metals from red mud and toxicity in human cells *in vitro*

Sanna Päivärinta-Antikainen [a,*], Marjo Huovinen [b], Satu Ojala [a], Lenka Matějová [c], Riitta L. Keiski [a], Kirsi H. Vähäkangas [b]

[a] *Environmental and Chemical Engineering, Faculty of Technology, University of Oulu, Oulu, Finland*
[b] *School of Pharmacy/Toxicology, Faculty of Health Sciences, University of Eastern Finland, Kuopio, Finland*
[c] *Institute of Environmental Technology, CEET, VŠB-Technical University of Ostrava, Ostrava, Czech Republic*

HIGHLIGHTS

- Elements leached from red mud decrease the viability of MCF-7 cells.
- Elements leached from red mud increase the formation of reactive oxygen species.
- Neutralization does not eliminate the toxicity of red mud.
- Acid activation increases the specific surface area of red mud.

GRAPHICAL ABSTRACT

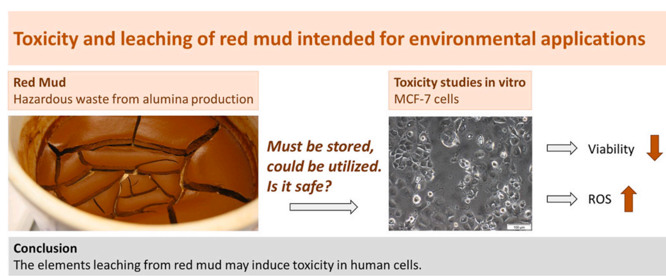

ARTICLE INFO

Handling Editor: X. Cao

Keywords:
Industrial waste
Acid activation
Cell toxicity
MCF-7 cells
MTT assay
Reactive oxygen species (ROS)

ABSTRACT

Toxicity of red mud, a waste from alumina production, was studied using human breast cancer MCF-7 cells. Culture medium was prepared by mixing water for 3 days with the red mud and removing solid particles afterwards (red mud water). Culture for 48 h of the cells in this medium in neutral pH decreased the cell viability, as analyzed by the MTT-test, and increased the formation of reactive oxygen species. Thus, neutralization does not eliminate the toxicity of red mud. In preliminary experiments, a combined effect of five metals (Cr, Li, V, Al, As) increased the formation of ROS (reactive oxygen species) statistically significantly. Each element separately did not have a similar effect. In environmental applications, red mud is likely to be used after activation. In this work, the red mud was activated using hydrochloric acid to study the physical and chemical properties before and after the treatment. Activation increased the specific surface area of red mud from 16 $m^2 g^{-1}$ to 148 $m^2 g{-}^1$, which is beneficial in many environmental applications such as in the adsorptive removal of pollutants. After activation, leaching of some elements from the red mud decreased (e.g. Al from 38.0 to 0.56 mg L^{-1}, As from 21.0 to 2.1 μg L^{-1}, V from 172.0 to 29.8 μg L^{-1}) while some increased (e.g. Li from 0.04 to 2.81 mg L^{-1}, Cr from 0.35 to 3.23 mg L^{-1}).

1. Introduction

Utilization of inorganic industrial and municipal waste and side streams, such as sludges, slags, and ashes, is an important and topical research field supporting the transition towards circular economy. These materials can potentially be used in many applications including

* Corresponding author. University of Oulu, Faculty of Technology, Environmental and Chemical Engineering, P.O. Box 4300, FI-90014, Oulu, Finland.
E-mail address: sanna.paivarinta-antikainen@oulu.fi (S. Päivärinta-Antikainen).

https://doi.org/10.1016/j.chemosphere.2023.138807
Received 29 December 2022; Received in revised form 26 April 2023; Accepted 27 April 2023
Available online 28 April 2023

construction materials (Sahu and Patel, 2016; Song et al., 2021; Wang et al., 2021), and even in environmental protection applications, such as catalysis and adsorption (Wang et al., 2008). The use of red mud and similar industrial side streams and wastes in environmental applications do not consume large amounts of these secondary materials, but they can still provide environmental and economic benefits by replacing pristine natural resources (Seelam et al., 2021).

Waste and side stream utilization also enhances the sustainability of different fields of industries and land construction. Plenty of research is focusing on the feasibility of secondary materials in different applications (Mohana et al., 2021; Nasier, 2021), however, it should be kept in mind that all three aspects of sustainability (economic, environmental and social) including the environmental and human health effects, should be considered when evaluating the utilization of the new waste and side-stream-based materials. Multidisciplinary research is thus very important.

Red mud, a bauxite residue, is a waste stream formed in the Bayer process, when aluminum oxide is produced from the bauxite ore (Alam et al., 2018). Red mud has strong alkalinity (pH 10–13) (Chen et al., 2022) and it contains heavy metals, rare earth elements (REEs) (Agrawal and Dhawan, 2021) and sometimes radioactive substances (Chen et al., 2023). Several studies have been conducted regarding the potential utilization of red mud, including metal recovery, use as a building material, a catalyst, in soil amendment and in wastewater treatment (Alam et al., 2018; Liu et al., 2011). Before the red mud can be stored or utilized in different applications, exposure assessment must be carried out, and the toxicity of the material to human and environmental health must be studied. People can get exposed to red mud in different ways, e.g., via the red mud dust spreading in the air near the reclamation areas or by getting exposed to the red mud containing sludge or water after rainwater leaching from reclamation to rivers, lakes, and groundwater, or after an accident (Liu et al., 2021a).

The most severe red mud accident occurred in 2010 in Ajka, Hungary, when ca. 0.7 million m^3 of red mud sludge flooded in the environment due to a collapsed tailings dam (Ruyters et al., 2011). Acute effects in humans were irritation of eyes and upper airways, and burn-like damage to tissues (Gundy et al., 2013). Genotoxicity was studied in the exposed people 4–6 weeks after the catastrophe, but no spontaneous or bleomycin-induced chromosomal aberrations in peripheral blood lymphocytes were seen (Gundy et al., 2013). However, these results do not rule out possible adverse chronic effects of red mud.

Long-term ecological effects of this disaster have also been studied (Winkler et al., 2018). Biological soil quality was found to be negatively affected due to the mixture of contaminants and it was stated that soil contaminated by red mud forms an unstable environment that is an under constant change (Winkler et al., 2018). In higher plants, red mud is genotoxic (Mišík et al., 2014). In the earthworm *Eisenia fetida*, red mud has been shown to cause oxidative stress and impaired reproduction (Hackenberger et al., 2019). However, more information on toxicity and mechanisms of toxicity in mammals is needed.

Risk evaluation of red mud use has been conducted by e.g. Arroyo et al. (2020) who studied the environmental risks regarding using red mud in bricks and determined the environmentally safe maximum amounts of RM replacing clay in bricks. Hou et al. (2021) state that using red mud in ultra-high performance concrete can provide a sustainable building material solution. Mukiza et al. (2019) have reviewed the use of red mud in road base and subgrade materials. They conclude that in addition to the suitable physical, mechanical and durability properties of red mud, additional research regarding e.g. leaching behavior of red mud in these applications is needed (Mukiza et al., 2019).

Keeping in mind the potential use of red mud derived materials in environmental applications, the potential toxicity of red mud needs to be studied further. In this paper, human MCF-7 breast cancer cells were used in the evaluation of toxicity of red mud. Justification for the use of these cells is that they are of human origin, they are easy to culture, and they retain their characteristics well in culture. In addition, this cell line is a well-characterized cell line which we have used successfully in toxicology studies before (Huovinen et al., 2015; Mohammed et al., 2020; Tampio et al., 2009). The work focuses especially on the elements that may leach from the red mud, or red mud derived products during their use for example in water purification applications or when red mud is stored. Studying the toxicity of red mud using human cells is novel. Results gained with human cells are more relevant considering toxicity on humans than results gained using cells from other species. Red mud activated by acid (Álvarez et al., 1999) has been used before in our studies as a catalyst (Päivärinta-Antikainen et al., 2023). This waste material can be used also in several other applications, such as adsorption (Wang et al., 2021). In addition to the toxicity studies, preliminary experiments were conducted to study whether activation of red mud would reduce leaching of toxic elements.

2. Materials and methods

2.1. Outline of the study

In this multidisciplinary study, methods of both toxicology and material research were used. The red mud sample received from a European alumina plant was filtered, washed, and dried before the delivery to Finland. The red mud was used to prepare red mud water for toxicity studies, in addition to using it as received and after drying or acid-activation (Pratt and Christoverson, 1982) in characterization and leaching studies (Fig. S1).

The most leached elements (see below) from the red mud as received or considered otherwise significant regarding the toxicity, were selected for the preliminary cell studies to prepare the model metal solutions. The toxicity of the red mud water and the prepared metal solutions was studied in human MCF–7 breast cancer cells. The cells were cultured in a Dulbecco's Modified Eagle medium (DMEM) 1) that was prepared in water mixed with red mud or 2) containing elements known to leach from the red mud or 3) as the control, containing only the normal ingredients for cell culture. As indicators of cell toxicity, cell viability by an MTT-test and the formation of reactive oxygen species (ROS) were analyzed.

Physical and chemical properties of the red mud as received and the activated red mud were compared using XRF (X-ray fluorescence), XRD (X-ray diffraction), nitrogen physisorption and FE-SEM (Field Emission Scanning Electron Microscope).

2.2. Preparation of red mud containing medium (DMEM-red mud-water)

There are no standard methods for the treatment of red mud to study the toxicity of leached compounds. Therefore, we developed a method, where first 50 g of red mud was mixed with 0.5 L ultrapure water (100 g L^{-1}) for 3 day at room temperature. After 2–3 h of settling, the water on top of the red mud sediment was removed using pipette and the supernatant was centrifuged (2000 rpm for 10 min) to separate the solids. Before the use in the cell culture medium, the pH of the red mud water was adjusted with HCl to ca. pH 7 and filtered with syringe filters (Supor (Hydrophilic polyethersulfone), Acrodisc®, 0.2 μm, Syringe Filter, Pall Life Sciences). Adjustment of pH ensures the living conditions for the cells and filtration removes contaminants (e.g., bacteria, yeast) that can disturb the growth of the cells. Exposure medium containing red mud water was prepared by dissolving DMEM as powder (13.5 g L^{-1}, Sigma, with 4.5 g L^{-1} glucose, L-glutamine, and sodium pyruvate) in the red mud water, with the following additions: 10 μg mL^{-1} gentamicin (Gibco), 0.375% $NaHCO_3$ (Gibco), 4.5 μg mL^{-1}insulin (Sigma-Aldrich) and 9% FBS (Sigma-Aldrich). Different dilutions of the DMEM-red mud-water for the cell culture were prepared by diluting the medium with pure DMEM. Pure DMEM was used as the control medium. Pure DMEM was prepared similarly but separately for the experiments with the red mud water (control medium I) and for the experiments with the model metal solutions (control medium II).

2.3. Elemental analysis of the red mud containing medium

The elemental composition of the DMEM-red mud-water at different stages of the preparation process was analyzed with ICP-MS. Liquid samples were diluted with 2.5% HNO_3 (TraceMetal™ grade, Fisher Chemical) before the measurements. Metal concentrations were analyzed using a PerkinElmer NexION 350D ICP-MS, USA device with the KED-mode. Multielement standard solution (TraceCERT® Periodic table mix 1 for ICP, Sigma-Aldrich) was used for the calibration. The elements analyzed were aluminum (Al), arsenic (As), beryllium (Be), calcium (Ca), cadmium (Cd), cobalt (Co), chromium (Cr), copper (Cu), iron (Fe), potassium (K), lithium (Li), magnesium (Mg), manganese (Mn), sodium (Na), nickel (Ni), phosphorus (P), lead (Pb), rubidium (Rb), vanadium (V), and zinc (Zn).

2.4. Model metal solutions

The model metal solutions were prepared for studying the effects of individual metals and their combinations on the viability of the MCF-7 cells. The most significant metals of the red mud leachate were selected based on the ICP-MS analysis of the prepared red mud exposure medium. Aluminum (Al), arsenic (As), chromium (Cr), lithium (Li) and vanadium (V) were the ones selected for these preliminary studies. The selection was done by comparing metal concentrations in the red mud leachate in different stages of the red mud medium preparation (Table 1) and selecting metals with the highest concentrations and the most potential harmful properties. Al was selected based on the high concentration in the original leachate. As and Cr are heavy metals and had also quite high leachability. The concentration of Li in the original leachate was rather high and it may have health effects on humans (Gitlin, 2016). Burke et al. (2012) studied red mud samples from the Ajka spill site in Hungary, and found that V in the samples was likely to be present as vanadium V^{5+} ion. In mammals, V^{5+} may be a reproductive and developmental toxicant (Domingo, 1996). The doses used were selected based on the concentrations measured from the red mud leachate in order to study the metal concentrations in the original leachate. The toxicity of each metal alone and two different combinations (Combination 1: Cr, Li and V, and Combination 2: Cr, Li, V, Al, As) were studied.

Chemicals used in the preparation of the model metal solutions were aluminum nitrate nonahydrate (98%, $Al(NO_3)_3·9H_2O$, Alfa Aesar), chromium(III) nitrate nonahydrate (98.5%, $Cr(NO_3)_3·9H_2O$, Alfa Aesar), sodium orthovanadate (99.9% (metals basis), Na_3VO_4, Alfa Aesar), sodium arsenate dibasic heptahydrate ($HAsNa_2O_4·7H_2O$, Sigma-Aldrich), and lithium nitrate ($LiNO_3$, Merck). Metal concentrations of the prepared metal containing mediums and their mixtures are presented in Table 1.

2.5. Cell experiments

2.5.1. Treatment of the cells

MCF-7 cells were sub-cultured on 48-well plates (50 000 cells/well) and the cells were grown for 24 h before the medium was changed to DMEM-RM-water for 48 h with various doses of the red mud (87 g L^{-1}, 43 g L^{-1}, 22 g L^{-1}, 9 g L^{-1}). Four replicates per dose on the same plate were used, and the experiments (MTT and ROS) were repeated on four different plates. In the preliminary experiments with the model metal solutions, the cells were cultured in metal containing media using metal concentrations presented in Table 1 (the analyzed concentrations in the single metal solutions: Al 61.6 mg L^{-1}, As 103 μg L^{-1}, Cr 0.52 mg L^{-1}, Li 79.1 μg L^{-1}, V 52 μg L^{-1}). With the model metal solutions, the MTT assay was repeated twice and the ROS measurement three times.

2.5.2. Measurement of cell viability (MTT assay)

The MTT assay is based on the conversion of 3-(4,5-dimethylthiazol-2-yl)-2,5-diphenyltetrazolium bromide (MTT) to insoluble formazan (Huovinen et al., 2015; Mosmann, 1983). Functional mitochondria can

Table 1
Concentrations of metals in the solutions at different stages of preparation of the red mud (RM) containing exposure medium (1.– 4.), concentrations of these metals in the control medium I (5.), the target concentrations in the model metal solutions (6.) and the measured metal concentrations in the model metal solution containing exposure mediums and their mixtures. Concentrations of the metals in the control medium of the model metal solution experiments (control medium II) are presented as a reference.

	As μg L^{-1}	Be μg L^{-1}	Cd μg L^{-1}	Co μg L^{-1}	Li μg L^{-1}	Pb μg L^{-1}	V μg L^{-1}	Al mg L^{-1}	Ca mg L^{-1}	Cr mg L^{-1}	Cu mg L^{-1}	Fe mg L^{-1}	K mg L^{-1}	Mg mg L^{-1}	Mn mg L^{-1}	Na mg L^{-1}	Ni mg L^{-1}	P mg L^{-1}	Rb mg L^{-1}	Zn mg L^{-1}
1. Non-filtrated RM water	94.5	0.0	4.7	1.6	98.6	4.1	478	73.3	1.9	0.67	0.02	2.18	9.3	1.4	0.06	151	0.09	3.5	0.01	<0.2
2. Non-filtrated, pH-adjusted (+sentrifuged) RM water	4.7	0.0	0.0	0.9	96.0	1.5	133	20.3	3.6	0.60	0.01	0.04	21.7	4.9	0.02	209	0.07	3.6	0.01	<0.2
3. Filtrated RM water (after pH adjustment)	4.9	0.0	1.2	0.3	101	0.5	48.1	0.5	1.4	0.50	0.01	0.10	10.3	1.8	0.00	150	0.07	1.9	0.01	<0.2
4. Exposure medium with RM water	7.9	2.7	3.0	2.4	78.3	1.8	46.5	0.9	45.0	0.44	0.04	0.34	299	31.7	0.02	4576	0.18	65.2	0.31	0.29
5. Control medium I	13.4	0.0	1.3	0.3	16.0	1.3	1.0	0.6	43.3	<0.05	0.05	0.36	293	25.7	0.01	4379	0.09	65.3	0.32	0.25
6. Target concentrations in metal solutions	100				80		50	70		1										
Al-solution	1.8				2.54		1.6	**61.6**		0.00										
As-solution	**103**				5.00		3.2	0.0		0.01										
Cr-solution	<1				1.41		<1	0.0		**0.52**										
Li-solution	<1				**79.1**		<1	0.0		0.00										
V-solution	<1				1.76		**52**	0.0		0.00										
Cr + Li + V	2				**84.9**		**52**	0.3		**0.52**										
Al + As + Cr + Li + V	**107**				**88.9**		**60**	**60.8**		**0.47**										
Control medium II	1.9				3.65		1.8	0.6		0.01										

convert MTT to purple colored formazan whereas damaged mitochondria lose this ability. The cells were cultured in DMEM-red mud-water or metal containing medium for 48 h after which the exposure medium was discarded, and the 0.5 mg mL^{-1} MTT-containing medium was pipetted in the wells. Incubation was continued at 37 °C for 2 h. Thereafter, the medium was removed, and formazan crystals were dissolved in SDS–DMF-buffer (pH 4.7). The absorbance of formazan was measured by an ELx 800 plate reader (Biotek Instruments, Inc.) at the wavelength of 570 nm. The measured absorbance is proportional to the number of viable cells and results were expressed as a percentage of the control.

2.5.3. Measurement of reactive oxygen species (ROS)

The production of reactive oxygen species (ROS) was measured with a 2′,7′-dichlorodihydrofluorescein diacetate (H_2DCFDA) method (Loikkanen et al., 2003; Tampio et al., 2009). The esterase activity in the cells results in the formation of water-soluble nonfluorescent 2′,7′-dichlorodihydrofluorescein (H_2DCF), which is rapidly oxidized in the presence of ROS to highly fluorescent 2′,7′-dichlorofluorescein (DCF). After a 48-h exposure to DMEM-red mud-water or metal containing medium, the exposure medium was replaced with the Hank's buffered salt solution (HBSS) loading buffer (137 mM NaCl, 1.3 mM $CaCl_2$, 5.4 mM KCl, 0.44 mM KH_2PO_4, 4.2 mM $NaHCO_3$, 0.34 mM Na_2HPO_4, 5.6 mM glucose, 10 mM HEPES, pH 7.4) containing 5 μM of H_2DCFDA. The cells were protected from light and incubated for 30 min at room temperature. DCF fluorescence (F_{ROS}) was measured with a VICTOR2 1420 multilabel plate reader (PerkinElmer, USA) at an excitation wavelength of 485 nm and an emission wavelength of 535 nm. After the measurement, 1.25 mM propidium iodide (PI) and 8.5 mM digitonin (DI) were added into each well and incubated for 20 min in the dark at room temperature. The fluorescence (F_{MAX}) was measured at an excitation wavelength of 531 nm and an emission wavelength of 615 nm. When calculating the results, background fluorescence was subtracted from the corresponding fluorescence values of the samples, and the values were then normalized to total cell number by dividing the DCF fluorescence values (F_{ROS}) by the maximum fluorescence values (F_{MAX}). The final value of ROS production was expressed as percentage of control. 3,4-Dichloroaniline (DCA) was used as a positive control in the ROS assay.

2.5.4. Statistical analysis

The cell viability and the ROS results are expressed as the mean ± SD (standard deviation). The statistical significance was analyzed with one-way ANOVA followed by the Dunnett's multiple comparison test in all comparisons. The statistics were conducted with GraphPad Prism 5.03 (Graph-Pad Prism software, San Diego, CA). The P values of <0.05 were considered as statistically significant.

2.6. Activation of red mud

Activated red mud (ARM) was prepared to represent an example of pre-treated red mud in this study. Activation of the red mud was conducted according to the dissolution/precipitation method originally developed by Pratt & Christoverson (Pratt and Christoverson, 1982). A 5 wt-% red mud mixture was prepared in distilled water and a sludge was formed via stirring. Next, 7.6% (Pratt & Christoverson (Pratt and Christoverson, 1982) 8 wt-%) of hydrochloric acid (HCl, ≥37%, Merck) was added and the mixture was boiled for 20 min under stirring. The volume of the mixture was then increased up to 1.3 L using distilled water (Pratt and Christoverson, 1982), and the pH was adjusted to 8 using ammonium hydroxide solution (Ammonia solution 25% for analysis, Merck). The suspension was kept at ~50 °C and stirred for 10 min. Red mud was filtered and washed with distilled water (40 °C, 3 × 50 mL). Finally, the resulting activated red mud was dried at 110 °C overnight and calcined at 500 °C for 2 h. The mass loss in calcination was ca. 8%. This material was used in the leaching experiments, and it was characterized with the same methods as the red mud as received.

2.7. Leaching and characterization of red mud

The leaching of elements from the red mud as received and the activated red mud was evaluated in preliminary batch experiments. 4 g of red mud or activated red mud was mixed with 40 mL of MilliQ water, resulting in solid-liquid ratio of 100 g L^{-1}. The sample bottles were agitated for three days. After this, the samples were settled and filtered before analyzing them with ICP-MS as described above. In the leaching experiments described here, also the sample red mud as received was studied again along with the ARM sample. The volume in the leaching experiments (4 g of red mud as received or ARM, 40 mL water) was different compared to the preparation of red mud water used in the toxicity experiments due to the limited amount of activated red mud available. The leaching properties of red mud as received and the activated red mud were compared in the experiment described here. The procedure used in this experiment was slightly different compared to the preparation of the red mud water. The leaching experiments of these preparations were carried out at the same time using the same equipment for both samples, and are thus comparable.

XRF (X-ray fluorescence) Spectrometer (PANalytical AXIOSmAX 4 kW PW2450 (Omnian software)) using a loose powder method was used for determining the chemical composition of the red mud samples.

XRD (X-ray diffraction) was applied for determining the crystalline phase composition of the samples. Rigaku SmartLab 9 kW with 40 kV and 135 mA X-Ray (with a rotating Co anode) was used. The scan speed was 4.0628°min^{-1}, step width 0.0200° and scan range from 5 to 130°. Analysis of the results was performed using the PDXL2 software with integrated access to the ICDD (International Center of Diffraction Data) PDF-4+ 2019 and 2021 RDB databases. Quantification of crystalline phases mass ratios was done with the Rietveld iterative method continued until the residual curve and Rwp values showed complete quantification.

Nitrogen physisorption measurements were performed using an ASAP2020 device (Micromeritics, USA). The specific surface area, S_{BET}, was calculated according to the classical Brunauer–Emmett–Teller (BET) theory for the $p/p_0 = 0.05–0.20$ including 8 points. The net pore volume, V_{net}, was determined from the nitrogen adsorption isotherm at relative pressure p/p_0 ~0.990. The mesopore-macropore-size distribution was evaluated from the adsorption branch of the nitrogen adsorption-desorption isotherm by the Barrett–Joyner–Halenda (BJH) method via the Roberts algorithm, using the BroekhoffdeBoer standard isotherm with the Faas correction and the assumption of the cylindrical-pore geometry (characterized by the diameter d_p of the pores).

High resolution images of the red mud samples were gained with a Field Emission Scanning Electron Microscope (FE-SEM; Zeiss SIGMA) using accelerating voltage of 5.0 kV. Analysis was conducted to obtain information on the surface textures of the red mud fractions.

3. Results and discussion

3.1. Cell viability and production of reactive oxygen species by red mud leachate (DMEM-red mud-water)

The two highest doses of the diluted red mud water decreased the viability of the MCF-7 cells statistically significantly (Fig. 1A). A dose-dependent decrease in the cell viability was seen in the MTT-test with the doses of 22–87 mg L^{-1}, and the calculated IC_{50} value (dose that will result in 50% decrease in viability of the cells) was 177.5 g L^{-1}. However, in the microscopic images the decrease in the cell viability was not clearly seen even with the highest dose (Fig. S2). The medium with the two highest doses of the red mud water also increased the production of reactive oxygen species (ROS) statistically significantly in the MCF-7 cells (Fig. 1B).

Our results on the elements leaching from the red mud reducing viability and increasing the formation of ROS in human MCF-7 breast cancer cells are in line with the decrease in viability and changes in the

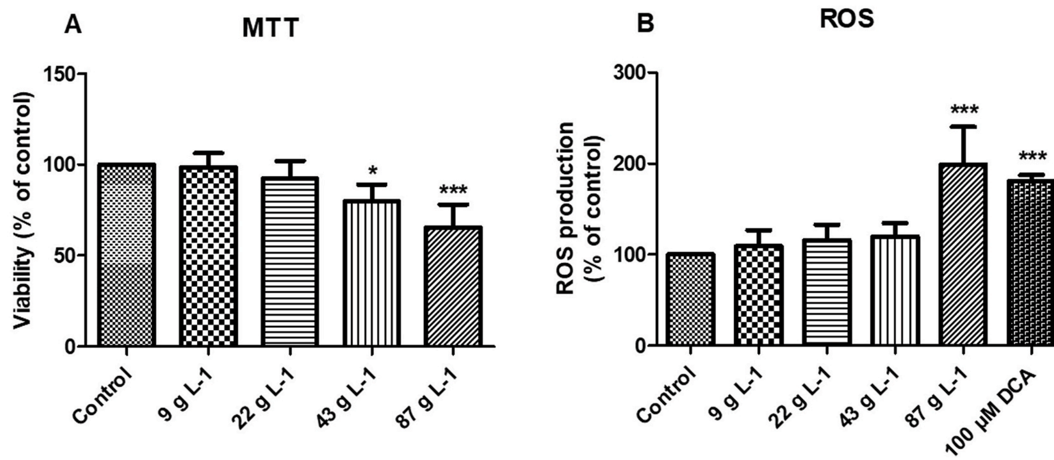

Fig. 1. Cell viability by MTT test (A) and the production of reactive oxygen species (ROS) (B) after 48-h culture of human breast cancer MFC-7 cells in various dilutions of the red mud water (water containing elements and compounds leached from red mud). Values are means ± SD of four individual experiments ($n = 4$) each mean of four replicates on the same 48-well plate; $^*p < 0.05$, $^{***}p < 0.001$ (compared to control). Oxidative 3,4-dichloroaniline (DCA) was used as a positive control in the ROS assay. The statistical significance was analyzed with one-way ANOVA followed by the Dunnett's multiple comparison test.

oxidative stress markers glutathione S-transferase and catalase in earthworm *Eisenia fetida* exposed to red mud from various origins (Hackenberger et al., 2019). Ecotoxicity of red mud has been widely studied (see Winkler et al., 2018), but potential human toxicity must also be thoroughly investigated. Possible effects of red mud exposure on human health are essential considering the various applications of red mud, e.g. adsorption and sewage treatment (Wang et al., 2021) possibly leading to human exposure.

Based on the analysis of the red mud containing water in different stages of the red mud medium preparation, concentrations of Co, Cr, Li, Mn and V were clearly higher in the exposure medium compared to the control medium. The Fe concentration in the exposure medium with the red mud water was lower than in the control medium without the red mud water.

The concentrations of several elements decreased in different stages, as was expected (Table 1). The concentrations of Al, As, Cr, Fe, Li and V all decreased when these elements, or compounds containing these elements were precipitated during the pH adjustment and filtration. Before filtration, the pH of the red mud water was ca. 11, which would have been too high for the cells. Also, possible contaminants, such as bacteria, were removed by filtration enabling uncontaminated cell culture. The concentration of As was a significant factor in the exposure medium at the non-filtered stage. However, it was significantly decreased during the pH-adjustment and filtering. Due to the somewhat surprisingly high As concentration of the control medium, the exposure medium with the red mud, contained a clearly lower As concentration compared to the control medium. The high As concentration in control medium can be partly explained by the analytical method used which is less sensitive for As and some other elements at the level of $\mu g\ L^{-1}$. Based on this, careful analysis of control media is always important.

In addition, other toxicants, such as NORM (naturally occurring radioactive material) (Qaidi et al., 2022) and REEs (rare-earth elements) (Agrawal and Dhawan, 2021), and elements such as Ti, Mo and Hg not analyzed in our water samples may have been present in the exposure medium. According to the XRF-analysis (Table S1), Ti was present in our undiluted, untreated red mud sample.

3.2. Cell viability and production of reactive oxygen species using model metal solutions

Cell viability and ROS production were studied in the cases of aluminum (Al), arsenic (As), chromium (Cr), lithium (Li), and vanadium (V) both individually and using two combinations (Combination 1: Cr, Li and V, and Combination 2: Cr, Li, V, Al, As). The used concentrations correspond to the ones of the non-filtrated red mud water (Table 1). With the model metal solutions, it is notable, that no effect on the cell viability was detected with single metals or with the two different mixtures (3 or 5 metals). However, a statistically significant increase in ROS production was detected with the mixture containing five metals (Cr, Li, V, Al and As) (Fig. 2). Thus, a mixture may be more toxic to MCF-7 cells than any of the metals alone. Combined effects are common in toxicology and can be very complex (Alexander et al., 2008). It has been found that the ROS formation has a role in the toxicity of both Al (Wu et al., 2012) and As (Hu et al., 2020). The results of this study do not exclude the possibility of Al and As increasing the formation of ROS in this study.

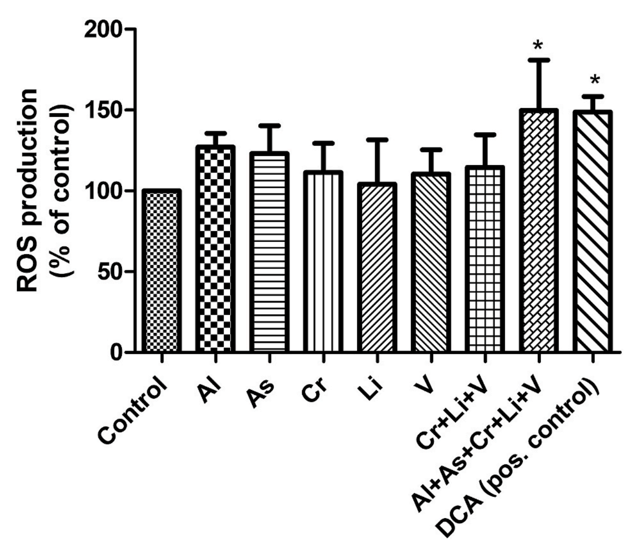

Fig. 2. Reactive oxygen species (ROS) production after 48 h of culture of human breast cancer MFC-7 cells in model metal solution containing medium. Final concentration of the metal in exposure medium is indicated. The values are mean ± SD from three individual experiments ($n = 3$) each mean of four replicates on the same 48-well plate; $^*p < 0.05$ (compared to control). In mixtures the doses of each metal were the same as in the experiment with a single metal. Oxidative 3,4-dichloroaniline (DCA) was used as a positive control. The statistical significance was analyzed with one-way ANOVA followed by the Dunnett's multiple comparison test.

3.3. Characterization and leaching of red mud samples

Red mud is a complex mixture of elements and the percental elemental composition of the red mud changed during the preparation of the activated red mud (Table 2). The dried red mud contains mostly Fe, Al, Na, Ca and Si. In the activated red mud, only three crystalline phases were identified with XRD (Table S1). These phases were hematite (Fe_2O_3), calcium and titanium containing perovskite ($CaTiO_3$) and rutile (TiO_2). The hematite content of the activated red mud was ca. 94%. Hematite was also the dominant phase in the dried red mud (47%). In the dried red mud also cancrinite ($Na_7Ca_{0.9}Al_6(SiO_4)_6(CO_3)_{1.4}(H_2O)_{2.1}$), katoite ($Ca_3Al_{3.5}O_{4.5}(OH)_{7.5}$), gibbsite ($Al(OH)_3$), calcium and titanium containing perovskite ($CaTiO_3$) and calcium carbonate ($Ca(CO_3)$) were identified. Cancrinite, katoite and gibbsite were transformed during the acid activation (removal of elements) and calcination (oxidation of hydroxides). Al compounds are assumed to be in an amorphous form in the activated red mud.

Elements regarded as the most significant, because of their known toxicity and relative abundance in the red mud water, were Al, As, Cr, Li and V. In the preliminary leaching experiments, concentration of Al and V in water was significantly lower after the acid activation (activated red mud compared to red mud as received) (Table 3). While leachability of V was also decreased in activation, it was still one of the most significant elements leaching based on the concentration and its potential toxicity. Information on the chemical form of species is crucial when evaluating the potential toxicity of vanadium and other elements leached from the red mud.

The concentration of Al was slightly increased, while the leachability of Al was drastically decreased after activation. Acid activation of the red mud transformed Al compounds to a less soluble form. The amounts of Na and Ca were significantly decreased by the activation. For Na, also the leachability was decreased, but in the case of Ca it was increased. Acid activation also decreased the leachability of As, K and Rb. However, there were a number of elements (Ca, Co, Cr, Li, Mg, Na, Ni, Sr and Zn) with increasing leachability after the acid activation. Ni and Sr are the most toxic ones of these elements (Burger and Lichtscheidl, 2019; Cohen-Solal, 2002; Genchi et al., 2020). Clearly Co (Leyssens et al., 2017), Ni (Das et al., 2018), and Sr (Pors Nielsen, 2004) may have human health effects based on earlier studies.

In environmental applications, e.g., in adsorption of contaminants from water, red mud could perform better in the form of activated red mud. Based on the results of the leaching experiments described above, the leaching of elements from the activated red mud might also be an issue and the activated red mud can not necessarily be seen as a safer material when it comes to the leaching of elements.

Table 2
Percentages (weight-%) of the most abundant elements in the dried red mud (Dried) and the acid activated red mud (ARM) determined with XRF (X-ray fluorescence).

	Dried	ARM
O	35.7	36.9
Fe	33.9	39.9
Al	7.4	9.0
Na	5.9	0.4
Ca	5.8	1.7
Si	5.7	6.1
Ti	3.5	4.1
P	0.6	0.6
Mn	0.3	0.3
Mg	0.3	0.1
Cl	0.1	0.1
Cr	0.1	0.1
Co	0.1	0.1
Ni	0.1	0.1
Zr	0.1	0.1
Pb	0.0	0.1

Table 3
Concentrations (μg L^{-1}) of the analyzed metals in two different red mud leachates. RM means red mud as received and ARM is the acid activated red mud sample.

	As μg L^{-1}	Be μg L^{-1}	Cd μg L^{-1}	Co μg L^{-1}	Cu μg L^{-1}	Ni μg L^{-1}	Pb μg L^{-1}	Rb μg L^{-1}	Sr μg L^{-1}	V μg L^{-1}	Zn μg L^{-1}	Al mg L^{-1}	B mg L^{-1}	Ca mg L^{-1}	Cr mg L^{-1}	Fe mg L^{-1}	K mg L^{-1}	Li mg L^{-1}	Mg mg L^{-1}	Mn mg L^{-1}	Na mg L^{-1}	P mg L^{-1}
RM	21.0	0.2	0.0	1.3	3.8	15.5	2.6	9.2	5.3	172.0	2.7	38.0	0.01	0.8	0.35	2.42	1.67	0.04	0.07	0.02	40.4	0.03
ARM	2.1	0.2	0.2	4.3	2.2	31.6	3.4	0.1	23.8	39.8	3.9	0.56	0.11	6.5	3.23	3.52	0.02	2.81	2.05	0.05	104.3	0.00

The dried red mud is a macroporous material showing a low specific surface area of 16 $m^2\ g^{-1}$. The activation changed the physical structure of red mud giving it a well-developed mesoporous structure, possessing higher specific surface area of 148 $m^2\ g^{-1}$ (Fig. 3A and B). Also, based on the FE-SEM images (Fig. 3C and D), the activated red mud is more porous and consists of smaller particles compared to the dried red mud. The net pore volume (V_{net}) of the dried red mud was 0.059 $cm^3_{liq}\ g^{-1}$and that of the activated red mud 0.247 $cm^3_{liq}\ g^{-1}$. A higher specific surface area is beneficial in many environmental applications (Albright's Chemical Engineering Handbook, 2008) and one of the goals of the pre-treatment was thus met.

3.4. Limitations of the study

The limitations of the study include studying only the toxicity of the elements leached from the red mud in neutral pH, while the high pH of the red mud is a significant factor regarding the hazardous nature of the material (Liu et al., 2021b; Ruyters et al., 2011). The model metal solution experiments were preliminary comprising of only a few metals studied in contrast to the very complex composition of the red mud. Red mud is known to contain hazardous trace elements including As, Pb, Hg, Cd and Cr (Wang and Liu, 2012). In addition, red mud is known to contain also naturally occurring radioactive material (NORM) (Goronovski et al., 2019; Qaidi et al., 2022) which were not analyzed in this study. The red mud/water -ratio used in the leachability tests was 100 g L^{-1} (100 kg m^{-3}). The bulk density of the original red mud varies between 800 and 1000 kg m^{-3} (Liu et al., 2021a). The starting material used had also been dried and pH-adjusted making it in many ways a different material compared to the original sludge. It is also important to note, that the composition of red mud varies globally (Liu et al., 2021b).

Studying the toxicity of activated red mud would be important in the future. Red mud is a complex mixture of different species and studying the effects of single metals does not give enough information on the toxicity of red mud. In toxicology, studying the combined effects of substances is both important and challenging (Andreas and Michael, 2018; Backhaus and Faust, 2012; Karri et al., 2016). Also, molecular mechanisms of toxicity of red mud would bring valuable information of the possible adverse human health effects.

4. Conclusions

The elements leaching from red mud may induce toxicity in human cells based on the decreased cell viability of human MCF-7 breast cancer cells and increased production of reactive oxygen species (ROS) in the *in vitro* experiments. Medium with red mud water was more toxic in the cells than any of the model metal solutions prepared. Only the combination of five metals (Cr, Li, V, Al and As) in the model solution induced statistically significant ROS formation. The concentrations of metals in the model metal solutions were higher than the concentrations of these metals in the red mud water and it can be concluded that the metals chosen for the model metal solutions are not alone responsible for the toxicity of the red mud water. The toxicity of the red mud, studied in neutral pH, is thus based on the combined effect of the analyzed elements and other compounds present in the red mud. Activation with acid improves the physical properties such as the specific surface area, which is beneficial when using the red mud for example as an adsorbent. Various pre-treatment methods can also be used to decrease the leaching of toxic elements. After activation, leaching of some elements from the

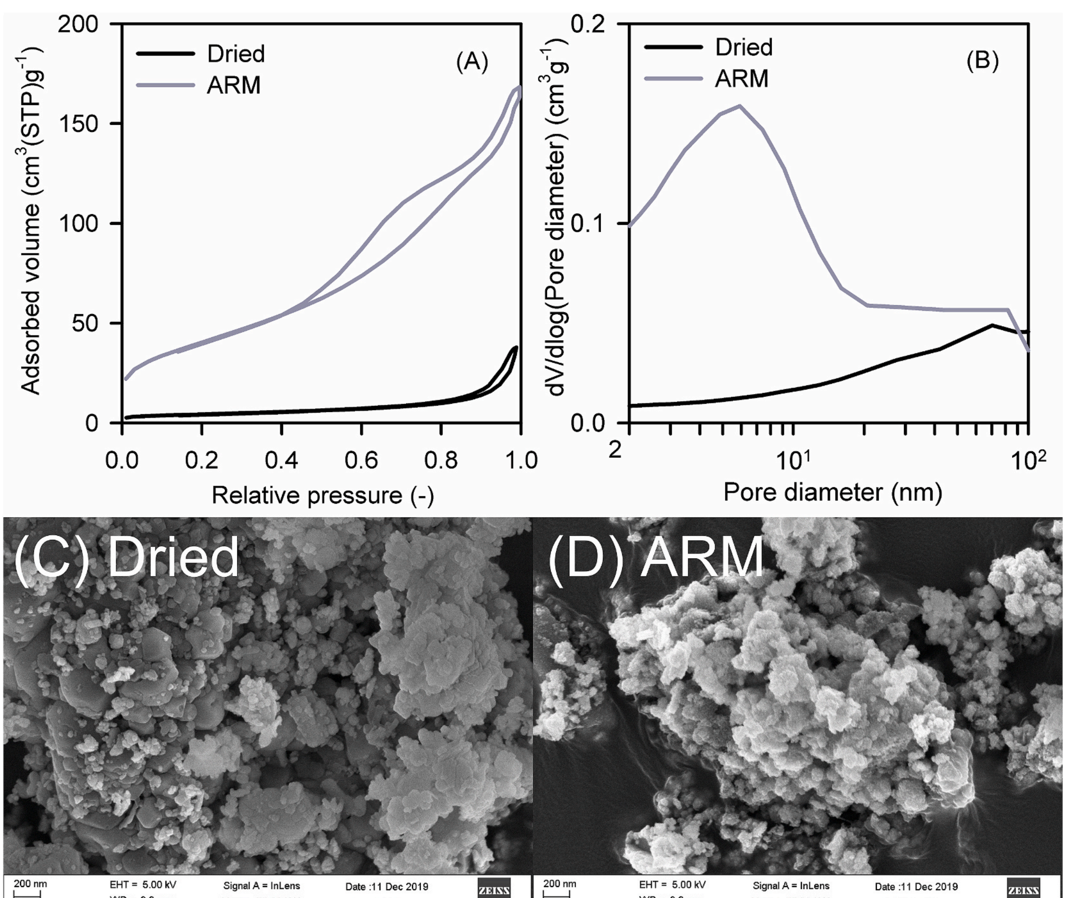

Fig. 3. Measured nitrogen adsorption-desorption isotherms (A) and evaluated pore-size distributions (B) of the dried red mud (Dried) and the acid activated red mud (ARM). FE-SEM images of the dried red mud (Dried, C) and the acid activated red mud (ARM, D).

red mud decreased (Al, As, K, Na, Rb and V) while others increased (Ca, Co, Cr, Li, Mg, Ni, Sr and Zn). It can thus be concluded that probably neither neutralization nor acid activation of red mud eliminate the negative health effects of the red mud exposure completely.

Credit author statement

Sanna Päivärinta-Antikainen: Conceptualization, Methodology, Formal analysis, Investigation, Writing – Original Draft, Writing – Review & Editing, Visualization, Funding acquisition. **Marjo Huovinen:** Conceptualization, Methodology, Formal analysis, Investigation, Writing – Original Draft, Writing – Review & Editing, Visualization. **Satu Ojala:** Conceptualization, Methodology, Formal analysis, Writing – Original Draft, Writing – Review & Editing, Supervision. **Lenka Matějová:** Formal analysis, Writing – Review & Editing, Visualization. **Riitta Keiski:** Resources, Writing – Review & Editing, Supervision, Project administration, Funding acquisition. **Kirsi Vähäkangas:** Conceptualization, Resources, Writing – Review & Editing, Supervision, Project administration.

Funding

Sanna Päivärinta-Antikainen: Emil Aaltonen Foundation, the North Ostrobothnia Regional Fund of the Finnish Cultural Foundation, the Finnish Cultural Foundation, and the University of Oulu Graduate School. The funding sources provided personal grants that have supported the different steps of the doctoral thesis work.

Declaration of competing interest

The authors declare that they have no known competing financial interests or personal relationships that could have appeared to influence the work reported in this paper.

Data availability

Data will be made available on request.

Acknowledgements

This work has been carried out with the financial support of Emil Aaltonen Foundation, the North Ostrobothnia Regional Fund of the Finnish Cultural Foundation, and the Finnish Cultural Foundation. The authors would like to thank the following persons at the University of Eastern Finland: Sirpa Peräniemi for the liquid sample analyzes and Pirjo Hänninen, Hannele Jaatinen, Jonna Niskanen and Jenni Küblbeck for practical help during the cell culture experiments. Part of this work was carried out with the support of the Center for Material Analysis, University of Oulu, Finland. University of Oulu Graduate School is acknowledged for supporting the research exchange financially. Lenka Matějová acknowledges the support of the project "COOPERATION" (project No. CZ.02.1.01./0.0/0.0/17_049/0008419) supported by ERDF and Large Research Infrastructure ENREGAT supported by MEYS of the Czech Republic (project No. LM2018098).

Appendix A. Supplementary data

Supplementary data to this article can be found online at https://doi.org/10.1016/j.chemosphere.2023.138807.

References

Agrawal, S., Dhawan, N., 2021. Evaluation of red mud as a polymetallic source – a review. Miner. Eng. 171, 107084 https://doi.org/10.1016/J.MINENG.2021.107084.
Alam, M.K., Zanganeh, J., Moghtaderi, B., 2018. The composition, recycling and utilisation of Bayer red mud. Resour. Conserv. Recycl. 141, 483–498. https://doi.org/10.1016/j.resconrec.2018.11.006.
Albright`s Chemical Engineering Handbook, 2008. CRC Press.
Alexander, J., Hetland, R.B., Vikse, R., Dybing, E., Sundstøl Eriksen, G., Farstad, W., Jenssen, B.M., Paulsen, J.E., Skåre, J.U., Steffensen, I.-L., Øvrebø, S., 2008. Combined toxic effects of multiple chemical exposures. In: VKM Report 2008: 16. Vitenskapskomiteen for mattrygghet/Norwegian Scientific Committee for Food Safety, pp. 17–24. https://vkm.no/download/18.d44969415d027c43cf1e869/1509708687404/Combined%20toxic%20effects%20of%20multiple%20chemical%20exposures.pdf.
Álvarez, J., Ordóñez, S., Rosal, R., Sastre, H., Dıez, F.V., 1999. A new method for enhancing the performance of red mud as a hydrogenation catalyst. Appl. Catal. Gen. 180, 399–409. https://doi.org/10.1016/S0926-860X(98)00373-1.
Andreas, K., Michael, F., 2018. Regulate to reduce chemical mixture risk. Science 361, 224–226. https://doi.org/10.1126/science.aat9219.
Arroyo, F., Luna-Galiano, Y., Leiva, C., Vilches, L.F., Fernández-Pereira, C., 2020. Environmental risks and mechanical evaluation of recycling red mud in bricks. Environ. Res. 186, 109537 https://doi.org/10.1016/J.ENVRES.2020.109537.
Backhaus, T., Faust, M., 2012. Predictive environmental risk assessment of chemical mixtures: a conceptual framework. Environ. Sci. Technol. 46, 2564–2573. https://doi.org/10.1021/es2034125.
Burger, A., Lichtscheidl, I., 2019. Strontium in the environment: review about reactions of plants towards stable and radioactive strontium isotopes. Sci. Total Environ. 653, 1458–1512. https://doi.org/10.1016/J.SCITOTENV.2018.10.312.
Burke, I.T., Mayes, W.M., Peacock, C.L., Brown, A.P., Jarvis, A.P., Gruiz, K., 2012. Speciation of arsenic, chromium, and vanadium in red mud samples from the Ajka spill site, Hungary. Environ. Sci. Technol. 46, 3085–3092. https://doi.org/10.1021/es3003475.
Chen, J., Wang, Y., Liu, Z., 2023. Red mud-based catalysts for the catalytic removal of typical air pollutants: a review. J. Environ. Sci. 127, 628–640. https://doi.org/10.1016/J.JES.2022.06.027.
Chen, W., Ding, Y., Li, B., Zhao, M., Li, C., Jiao, Y., 2022. Pyrolysis characteristics and stage division of red mud waste from the alumina refining process for cyclic utilization. Fuel 326, 125063. https://doi.org/10.1016/J.FUEL.2022.125063.
Cohen-Solal, M., 2002. Strontium overload and toxicity: impact on renal osteodystrophy. Nephrol. Dial. Transplant. 17 (Suppl. 2), 30–34. https://doi.org/10.1093/ndt/17.suppl_2.30.
Das, K.K., Reddy, R.C., Bagoji, I.B., Das, S., Bagali, S., Mullur, L., Khodnapur, J.P., Biradar, M.S., 2018. Primary concept of nickel toxicity - an overview. J. Basic Clin. Physiol. Pharmacol. 30, 141–152. https://doi.org/10.1515/jbcpp-2017-0171.
Domingo, J.L., 1996. Vanadium: a review of the reproductive and developmental toxicity. Reprod. Toxicol. 10, 175–182. https://doi.org/10.1016/0890-6238(96)00019-6.
Genchi, G., Carocci, A., Lauria, G., Sinicropi, M.S., Catalano, A., 2020. Nickel: human health and environmental toxicology. Int. J. Environ. Res. Publ. Health. https://doi.org/10.3390/ijerph17030679.
Gitlin, M., 2016. Lithium side effects and toxicity: prevalence and management strategies. Int. J. bipolar Disord. 4, 27. https://doi.org/10.1186/s40345-016-0068-y.
Goronovski, A., Vind, J., Vassiliadou, V., Panias, D., Tkaczyk, A.H., 2019. Radiological assessment of the Bayer process. Miner. Eng. 137, 250–258. https://doi.org/10.1016/J.MINENG.2019.04.016.
Gundy, S., Farkas, G., Székely, G., Kásler, M., 2013. No short-term cytogenetic consequences of Hungarian red mud catastrophe. Mutagenesis 28, 1–5. https://doi.org/10.1093/mutage/ges042.
Hackenberger, D.K., Feigl, V., Lončarić, Ž., Hackenberger, B.K., 2019. Biochemical and reproductive effects of red mud to earthworm Eisenia fetida. Ecotoxicol. Environ. Saf. 168, 279–286. https://doi.org/10.1016/j.ecoenv.2018.10.097.
Hou, D., Wu, D., Wang, X., Gao, S., Yu, R., Li, M., Wang, P., Wang, Y., 2021. Sustainable use of red mud in ultra-high performance concrete (UHPC): design and performance evaluation. Cem. Concr. Compos. 115, 103862 https://doi.org/10.1016/J.CEMCONCOMP.2020.103862.
Hu, Y., Li, J., Lou, B., Wu, R., Wang, G., Lu, C., Wang, H., Pi, J., Xu, Y., 2020. The role of reactive oxygen species in arsenic toxicity. Biomolecules 10. https://doi.org/10.3390/biom10020240.
Huovinen, M., Loikkanen, J., Naarala, J., Vahakangas, K., 2015. Toxicity of diuron in human cancer cells. Toxicol. Vitro 29, 1577–1586. https://doi.org/10.1016/j.tiv.2015.06.013.
Karri, V., Schuhmacher, M., Kumar, V., 2016. Heavy metals (Pb, Cd, as and MeHg) as risk factors for cognitive dysfunction: a general review of metal mixture mechanism in brain. Environ. Toxicol. Pharmacol. 48, 203–213. https://doi.org/10.1016/j.etap.2016.09.016.
Leyssens, L., Vinck, B., Van Der Straeten, C., Wuyts, F., Maes, L., 2017. Cobalt toxicity in humans-A review of the potential sources and systemic health effects. Toxicology 387, 43–56. https://doi.org/10.1016/j.tox.2017.05.015.
Liu, X., Han, Y., He, F., Gao, P., Yuan, S., 2021a. Characteristic, hazard and iron recovery technology of red mud - a critical review. J. Hazard Mater. 126542 https://doi.org/10.1016/J.JHAZMAT.2021.126542.
Liu, X., Han, Y., He, F., Gao, P., Yuan, S., 2021b. Characteristic, hazard and iron recovery technology of red mud - a critical review. J. Hazard Mater. 420, 126542 https://doi.org/10.1016/J.JHAZMAT.2021.126542.
Liu, Y., Naidu, R., Ming, H., 2011. Red mud as an amendment for pollutants in solid and liquid phases. Geoderma 163, 1–12. https://doi.org/10.1016/j.geoderma.2011.04.002.
Loikkanen, J., Naarala, J., Vähäkangas, K.H., Savolainen, K.M., 2003. Glutamate increases toxicity of inorganic lead in GT1-7 neurons: partial protection induced by flunarizine. Arch. Toxicol. 77, 663—671. https://doi.org/10.1007/s00204-003-0498-z.

Mišík, M., Burke, I.T., Reismüller, M., Pichler, C., Rainer, B., Mišíková, K., Mayes, W.M., Knasmueller, S., 2014. Red mud a byproduct of aluminum production contains soluble vanadium that causes genotoxic and cytotoxic effects in higher plants. Sci. Total Environ. 493, 883–890. https://doi.org/10.1016/J.SCITOTENV.2014.06.052.

Mohammed, A.M., Huovinen, M., Vähäkangas, K.H., 2020. Toxicity of diuron metabolites in human cells. Environ. Toxicol. Pharmacol. 78, 103409 https://doi.org/10.1016/j.etap.2020.103409.

Mohana, R., Prabavathy, S., Leela Bharathi, S.M., 2021. Sustainable utilization of industrial wastes for the cleaner production of ferrocement structures: a comprehensive review. J. Clean. Prod. 291, 125916 https://doi.org/10.1016/J.JCLEPRO.2021.125916.

Mosmann, T., 1983. Rapid colorimetric assay for cellular growth and survival: application to proliferation and cytotoxicity assays. J. Immunol. Methods 65, 55–63. https://doi.org/10.1016/0022-1759(83)90303-4.

Mukiza, E., Zhang, L.L., Liu, X., Zhang, N., 2019. Utilization of red mud in road base and subgrade materials: a review. Resour. Conserv. Recycl. 141, 187–199. https://doi.org/10.1016/J.RESCONREC.2018.10.031.

Nasier, S., 2021. Utilization of recycled form of concrete, E-wastes, glass, quarry rock dust and waste marble powder as reliable construction materials. Mater. Today Proc. 45, 3231–3234. https://doi.org/10.1016/J.MATPR.2020.12.381.

Päivärinta-Antikainen, S., Ojala, S., Pitkäaho, S., Matějová, L., Keiski, R.L., 2023. On the utilization of modified red mud in dimethyl disulfide and methyl mercaptan emission abatement. Resources. https://doi.org/10.3390/resources12010009.

Pors Nielsen, S., 2004. The biological role of strontium. Bone 35, 583–588. https://doi.org/10.1016/J.BONE.2004.04.026.

Pratt, K.C., Christoverson, V., 1982. Hydrogenation of a model hydrogen-donor system using activated red mud catalyst. Fuel 61, 460–462.

Qaidi, S.M.A., Tayeh, B.A., Ahmed, H.U., Emad, W., 2022. A review of the sustainable utilisation of red mud and fly ash for the production of geopolymer composites. Construct. Build. Mater. 350, 128892 https://doi.org/10.1016/J.CONBUILDMAT.2022.128892.

Ruyters, S., Mertens, J., Vassilieva, E., Dehandschutter, B., Poffijn, A., Smolders, E., 2011. The red mud accident in Ajka (Hungary): plant toxicity and trace metal bioavailability in red mud contaminated soil. Environ. Sci. Technol. 45, 1616–1622. https://doi.org/10.1021/es104000m.

Sahu, M.K., Patel, R.K., 2016. Methods for utilization of red mud and its management. Environ. Mater. Waste 485–524. https://doi.org/10.1016/B978-0-12-803837-6.00019-6.

Seelam, P.K., Sreenivasan, H., Ojala, S., Pitkäaho, S., Laitinen, T., Niu, H., Keiski, R.L., Illikainen, M., 2021. Modified geopolymers as promising catalyst supports for abatement of dichloromethane. J. Clean. Prod. 280, 124584 https://doi.org/10.1016/J.JCLEPRO.2020.124584.

Song, Q., Guo, M.-Z., Wang, L., Ling, T.-C., 2021. Use of steel slag as sustainable construction materials: a review of accelerated carbonation treatment. Resour. Conserv. Recycl. 173, 105740 https://doi.org/10.1016/J.RESCONREC.2021.105740.

Tampio, M., Markkanen, P., Puttonen, K.A., Hagelberg, E., Heikkinen, H., Huhtinen, K., Loikkanen, J., Hirvonen, M.-R., Vahakangas, K.H., 2009. Induction of PUMA-alpha and down-regulation of PUMA-beta expression is associated with benzo(a)pyrene-induced apoptosis in MCF-7 cells. Toxicol. Lett. 188, 214–222. https://doi.org/10.1016/j.toxlet.2009.04.016.

Wang, P., Liu, D.-Y., 2012. Physical and chemical properties of sintering red mud and bayer red mud and the implications for beneficial utilization. Mater. https://doi.org/10.3390/ma5101800.

Wang, S., Ang, H.M., Tadé, M.O., 2008. Novel applications of red mud as coagulant, adsorbent and catalyst for environmentally benign processes. Chemosphere 72, 1621–1635. https://doi.org/10.1016/j.chemosphere.2008.05.013.

Wang, S., Jin, H., Deng, Y., Xiao, Y., 2021. Comprehensive utilization status of red mud in China: a critical review. J. Clean. Prod. 289, 125136 https://doi.org/10.1016/J.JCLEPRO.2020.125136.

Winkler, D., Bidló, A., Bolodár-Varga, B., Erdő, Á., Horváth, A., 2018. Long-term ecological effects of the red mud disaster in Hungary: regeneration of red mud flooded areas in a contaminated industrial region. Sci. Total Environ. 644, 1292–1303. https://doi.org/10.1016/J.SCITOTENV.2018.07.059.

Wu, Z., Du, Y., Xue, H., Wu, Y., Zhou, B., 2012. Aluminum induces neurodegeneration and its toxicity arises from increased iron accumulation and reactive oxygen species (ROS) production. Neurobiol. Aging 33, 199. https://doi.org/10.1016/j.neurobiolaging.2010.06.018 e1–12.